

N65-29465

(ACCESSION NUMBER)

27

(PAGES)

TMX-51975

(NASA CR OR TMX OR AD NUMBER)

(THRU)

1

(CODE)

09

(CATEGORY)

GPO PRICE

\$

CFSTI PRICE(S)

\$

Hard copy (HC)

2.00

Microfiche (MF)

.50

ff 653 July 65

Current Distribution in a Thin Film
Superconducting Strip Transmission Line

A. R. SASS

RCA Laboratories
Radio Corporation of America
Princeton, New Jersey

and

I. D. SKURNICK

Lewis Research Center
National Aeronautics & Space Administration
Cleveland, Ohio

ABSTRACT

29465

In the long wavelength limit the current distribution in a thin film superconducting strip transmission line can be described by an inhomogeneous Fredholm equation of the second kind. By considering a fluxoid conservation derivation of this equation, physical insight into the structure of the kernel follows naturally. An approximate analytic solution to the integral equation is derived for a specified range of geometrical parameters commonly encountered in practice. The solution is obtained by making use of the Liouville-Neumann method of successive iterations and approximating the resulting series by a series involving powers of a defined coupling factor. It is shown that the critical current of the thin film superconducting strip transmission line, based on the calculations in the paper and a critical current density hypothesis, is underestimated by less than 5%.

Author

INTRODUCTION

Several authors have indicated that superconductive computer components which are constructed in the form of thin film strip transmission lines are advantageous from the standpoint of switching speed and miniaturization.¹⁻⁶

Superconducting strip transmission lines are also useful in the transportation of electrical information within a superconducting computer due to inherent negligible loss characteristics and high group velocity.^{2,5} The latter is true only if the film thickness is larger than, or comparable to, the London penetration depth. It has also been shown that if the film thickness is less than the penetration depth the group velocity is appreciably decreased, making the strip line useful for ~~delay~~ line memory application.² In all the above devices it would be useful to be able to predict the total current which can be carried by the strip line before it becomes normally conducting.

Several microscopic theories have been advanced which indicate that switching in a thin film is initiated by a critical current density.⁷ Cooper and Marcus have shown, independently, that the problem of thin film switching is complicated by the fact that the current density is not constant over the cross-section of the film.^{8,9} Using a formal Green's function approach, and employing the London current-field relation, Cooper derived the general inhomogeneous (integral) Fredholm equation of the second kind describing the current density distribution in a single film. He also obtained a specialized equation for the case in which the film thickness is less than or equal to the penetration depth - the thin film case. Marcus derived an identical equation by combining the Biot-Savart law and London's equation, and obtained computer solutions for the thin film case. The above methods can be used to derive an integral equation for the case of a strip transmission line. Due to the complexity of the kernel, analytic solutions

to the integral equation have not been found to date for either the single film or strip line cases.

It is shown below that when the integral equation is derived for the strip transmission line, using the concept of fluxoid conservation explicitly, certain useful properties of the kernel can be readily deduced. These properties allow the approximate evaluation of the Liouville-Neumann series for a range of geometric parameters of practical interest. The analytic solution ^{for} of the current density distribution in the strip line exhibits the same property of current peaking at the film edges that Cooper and Marcus found for the single film. The critical current of the system can be calculated from a knowledge of the current density in the strip line and the critical current density obtained from microscopic theory, and/or independent experimentation.

STATEMENT OF PROBLEM

Consider the transmission line structure in the form of two parallel cylindrical conductors shown in Fig. 1. For the sake of generality it is assumed, at first, that the cross-section of each conductor is arbitrary. It is further assumed that the wavelength of the fields propagating along the structure is much larger than the transverse dimensions of the structure so that a static analysis is valid. It is also assumed that the current density is in the z-direction and therefore is only a function of x and y. The latter condition is necessary in order to satisfy charge conservation for this quasi-static case ($\nabla \cdot \mathbf{J} \approx 0$).

The derivation of the equation describing the current distribution in the conductors is equally valid for the cases in which: (1) the conductors are both normally conducting, (2) one conductor is superconducting and the other is normally

conducting, and (3) both conductors are superconducting. It is advantageous to first consider the classic case in which both cylinders are normally conducting.

Since $\vec{J} = \sigma \vec{E}$ in both conductors, applying Faraday's law to the dotted contour shown in Fig. 1 yields,

$$J(\vec{r}) - J(0) = \sigma \mu_0 \frac{d}{dt} \int_0^{\vec{r}} \vec{H}(\vec{r}') \cdot [\hat{a}_z \times d\vec{r}'] \quad (1)$$

in rationalized mks units. \vec{r} is the usual position vector in the x-y plane, \hat{a}_z is a unit vector in the z-direction, and $d\vec{r}$ is a differential vector line element of integration. $\vec{H}(\vec{r})$ is the magnetic field intensity generated by current elements in both conductors. For the static case, the right-hand side of Eq. (1) is zero and therefore the current distribution in each conductor is uniform. It is interesting to note that the distribution in conductor 1 is uniform even if conductor 2 does not have a uniform distribution (for instance if conductor 2 is a superconductor - this case is described below), as long as conductor 1 is normally conducting.

For the case in which both conductors are perfectly conducting ($\sigma = \infty$), the right-hand side of Eq. (1) is still zero in the static situation. However, at some time in the past a transient existed so that it appears that infinite current densities were generated. This unrealistic situation is alleviated by stipulating that during the transient and afterwards the current flows in an infinitely thin layer at the perfect conductor surfaces with a distribution such that \vec{H} is time independent everywhere inside the body of the conductor. Starting from zero initial conditions it is evident that \vec{H} is zero everywhere inside of the cylinders. This is guaranteed by stipulating that there is no component of \vec{H} perpendicular to the conductor's surface. Thus, if \vec{r}_{s1} and \vec{r}_{s2} are the position vectors denoting the surface of conductors 1 and 2 respectively and $\vec{J}_w(\vec{r}_s)$ is the

current per unit width at the conductor surface, then $\bar{J}_w(\vec{r}_s)$ is the solution to the coupled integral equations

$$\int_{\text{I}} \frac{\bar{J}_w(\vec{r}'_{s1}) [\hat{a}_z \times (\vec{r}_{s1} - \vec{r}'_{s1}) \cdot \hat{a}'_{\perp}] d\ell'_{s1}}{2\pi |\vec{r}_{s1} - \vec{r}'_{s1}|^2} - \int_{\text{II}} \frac{\bar{J}_w(\vec{r}'_{s2}) [\hat{a}_z \times (\vec{r}_{s1} - \vec{r}'_{s2}) \cdot \hat{a}'_{\perp}] d\ell'_{s2}}{2\pi |\vec{r}_{s1} - \vec{r}'_{s2}|^2} = 0 \quad (2)$$

$$\int_{\text{I}} \frac{\bar{J}_w(\vec{r}'_{s1}) [\hat{a}_z \times (\vec{r}_{s2} - \vec{r}'_{s1}) \cdot \hat{a}'_{\perp}] d\ell'_{s1}}{2\pi |\vec{r}_{s2} - \vec{r}'_{s1}|^2} - \int_{\text{II}} \frac{\bar{J}_w(\vec{r}'_{s2}) [\hat{a}_z \times (\vec{r}_{s2} - \vec{r}'_{s2}) \cdot \hat{a}'_{\perp}] d\ell'_{s2}}{2\pi |\vec{r}_{s2} - \vec{r}'_{s2}|^2} = 0$$

While Eqs. (2) will not be solved here, some useful information can be obtained from their form and is summarized below:

- (1) The magnetic flux through any imaginary surface in the interior of either conductor is zero.
- (2) The surface current distribution in conductor 1 is influenced by the cross-sectional shape of conductor 1, conductor 2, and the separation between them.
- (3) The surface current distribution in conductor 1 is altered if conductor 2 does not carry the same total current as conductor 1. The distribution in conductor 1 is altered by the presence of conductor 2 even if conductor 2 carries zero net current.

The static case in which $\sigma = \infty$ can be simulated by a dynamic situation in which the skin depth is much less than the transverse dimensions of the conductor.

Consider the case in which both conductors are superconducting. In this situation $\vec{E} = \mu_0 \beta^{-2} \frac{\partial \vec{J}}{\partial t}$ in each of the cylinders, where β^{-1} is the London penetration depth. Thus, instead of Eq. (1), it can be shown that

$$\frac{d}{dt} [J(\vec{r}) - J(0) - \beta^2 \int_0^r \vec{H}(\vec{r}') \cdot (\hat{a}_z \times d\vec{r}')] = 0 \quad (3)$$

The quantity within the brackets in Eq. (3) is the London fluxoid. Thus Eq. (3)

expresses the principle of fluxoid conservation. Starting from the London zero field initial conditions, it is seen that the fluxoid associated with this or any other contour within the superconducting cylinder is zero. This is the exact analog of the zero flux condition encountered in the case of perfect conductors. Conditions 2 and 3 which were stated for perfect conductors remain the same for superconductors except that the word "surface" must be deleted. This is apparent since the infinite current density situation associated with a time rate of change of flux no longer exists in this case.

It is convenient at this point to introduce the vector potential defined by the equation

$$\vec{H} = \mu_0^{-1} \nabla \times \vec{A} \quad (4a)$$

All calculations will be carried out in the Coulomb gauge. Furthermore \vec{A} is chosen such that it is in the z-direction and thus is only a function of x and y. Thus in the cylinders

$$\vec{H}(\vec{r}) = -\nabla \times \left[\frac{\hat{a}_z}{2\pi} \int_{S_I+S_{II}} J(\vec{r}') \ln |\vec{r} - \vec{r}'| d^2\vec{r}' \right] \quad (4b)$$

where the integration in Eq. (4b) is over the cross-sectional areas of both conductors. Using the identity

$$\vec{H}(\vec{r}) \cdot (\hat{a}_z \times d\vec{r}) = \frac{1}{2\pi} \frac{\partial}{\partial r} \int_{S_I+S_{II}} J(\vec{r}') \ln |\vec{r} - \vec{r}'| d^2\vec{r}' dr \quad (5)$$

and the fact that the fluxoid is zero yields

$$J(\vec{r}) = J(0) - \frac{\beta^2}{2\pi} \int_{S_I+S_{II}} J(\vec{r}') \ln |\vec{r}'| d^2\vec{r}' + \frac{\beta^2}{2\pi} \int_{S_I+S_{II}} J(\vec{r}') \ln |\vec{r}-\vec{r}'| d^2\vec{r}' \quad (6a)$$

Eq. (6a) is identical to that derived by Cooper and Marcus. The first two terms on the right-hand side in Eq. (6a) are independent of \vec{r} , therefore the current density can be expressed as

$$J(\vec{r}) = C + \frac{\beta^2}{2\pi} \int_{S_I + S_{II}} J(\vec{r}') \ln |\vec{r} - \vec{r}'| d^2 \vec{r}' \quad (6b)$$

where C is an arbitrary constant determined by the total current.

Using the concepts introduced in the above derivation the following interesting fact is apparent: The nonuniformity of the current density in the film ($J(\vec{r}) \neq J(0)$, $\vec{r} \neq 0$) is due to the magnetic flux crossing the plane surrounded by the dotted contour shown in Fig. 1. For certain cross-sectional geometries (such as the strip transmission line which will be discussed later) this flux is small if both conductors carry equal and opposite currents. Thus, in these cases, only small variations of the current density are expected. Furthermore, in the case of a strip transmission line, this concept allows certain properties of the kernel of the integral equation to be deduced so that a closed form solution to Eq. (6b) can be demonstrated.

Before proceeding to this solution, consider the case in which conductor 1 is superconducting and conductor 2 is normally conducting. As was shown previously, the current density in the normal conductor is uniform, so that if $I_{1,2}$ and $A_{1,2}$ are the net currents and cross-sectional areas of conductors 1 and 2 respectively, Eq. (6a) becomes

$$J(\vec{r}) - J(0) = \frac{\beta^2}{2\pi} \int_{S_I} J(\vec{r}') \ln |\vec{r} - \vec{r}'| d^2 \vec{r}' - \frac{\beta^2}{2\pi} \int_{S_I} J(\vec{r}') \ln |\vec{r}'| d^2 \vec{r}' \quad (7)$$

$$+ \frac{\beta^2 I_2}{2\pi A_2} \int_{S_{II}} \ln |\vec{r} - \vec{r}'| d^2 \vec{r}' - \frac{\beta^2 I_2}{2\pi A_2} \int_{S_{II}} \ln |\vec{r}'| d^2 \vec{r}' .$$

It is interesting to note that for this case the distribution in conductor 1 is not influenced by the presence of conductor 2 for $I_2 = 0$. This was not true for the case of two perfect conductors or two superconductors, as was shown above.

STRIP TRANSMISSION LINE OF RECTANGULAR CROSS SECTION

Consider the strip transmission line, shown in Fig. 2, consisting of two parallel, infinitely long, superconducting thin films of rectangular cross-section. Each is of width W and thickness d , and the two are separated by a distance ℓ . The parameters of the system are chosen to be in a range of practical interest denoted by $.0001 \leq \frac{d}{W} \leq .01$, $(\beta d) \leq 1$, and $\frac{1}{K} \frac{\ell}{d} < 6$. A current, I_0 , flows into the top film, and an equal but oppositely directed current flows in the bottom film. For the case of the strip transmission line system described above, Eq. (6b) becomes

$$J(x,y) = C + \frac{\beta^2}{2\pi} \left[\int_{-\frac{W}{2}}^{+\frac{W}{2}} \int_{-\frac{d}{2}}^{+\frac{d}{2}} J(x',y') \ln \left| (x-x')^2 + (y-y')^2 \right| dx' dy' + \int_{-\frac{W}{2}}^{+\frac{W}{2}} \int_{-\frac{d}{2}-\ell}^{\frac{d}{2}-\ell} J(x',y') \ln \left| (x-x')^2 + (y-y')^2 \right| dx' dy' \right] \quad (8a)$$

$$\int_{-\frac{W}{2}}^{+\frac{W}{2}} \int_{-\frac{d}{2}-\ell}^{\frac{d}{2}-\ell} J(x',y') \ln \left| (x-x')^2 + (y-y')^2 \right| dx' dy'$$

Using the change of variables $x' \rightarrow (x' + \ell)$ in the last integral on the right-hand side in Eq. (8a), and noting that

$$J(x,y) \Big|_{-\frac{d}{2} < x < \frac{d}{2}} = -J(-x-\ell, y) \Big|_{-\frac{d}{2} < x < \frac{d}{2}} \quad (8b)$$

yields

$$J(x,y) = C + \frac{\beta^2}{4\pi} \int_{-\frac{W}{2}}^{+\frac{W}{2}} \int_{-\frac{d}{2}}^{+\frac{d}{2}} J(x',y') \ln \frac{|(x-x')^2 + (y-y')^2|}{|(x+x'+\ell)^2 + (y-y')^2|} dx' dy' \quad (9)$$

Since $(\beta d) \leq 1$ it will be assumed that J does not vary appreciably in the x -direction in the film. (This assumption will be examined more closely in the next section.)

Therefore $J(x,y) \approx J(0,y) = J(y)$ and Eq. (9) becomes, after introducing the dimensionless variable $u = (2/W)y$,

$$J(u) = C + \frac{(\beta d)^2 (W/d)}{8\pi} \int_{-1}^{+1} J(u') K(u,u') du' \quad (10a)$$

where $K(u,u') = K(|u-u'|) =$

$$\begin{aligned} &= \ln \left| (d/W)^2 + (u-u')^2 \right| + 2 \left(\frac{u-u'}{d/W} \right) \tan^{-1} \left(\frac{d/W}{u-u'} \right) + \\ &+ \left(\frac{1}{d} \right) \left\{ \left(\ell - \frac{d}{2} \right) \ln \left| \left(2 \frac{\ell}{W} - \frac{d}{W} \right)^2 + (u-u')^2 \right| - \left(\ell + \frac{d}{2} \right) \ln \left| \left(2 \frac{\ell}{W} + \frac{d}{W} \right)^2 + (u-u')^2 \right| \right\} + \\ &+ \left(\frac{u-u'}{d/W} \right) \left\{ \tan^{-1} \left(\frac{2 \frac{\ell}{W} - \frac{d}{W}}{u-u'} \right) - \tan^{-1} \left(\frac{2 \frac{\ell}{W} + \frac{d}{W}}{u-u'} \right) \right\}. \end{aligned} \quad (10b)$$

The kernel of the integral equation is an explicit function of the thickness to width ratio of the films, as well as the ratio of the separation distance to the width. It was mentioned earlier that the nonuniformity of the current density is due to the magnetic flux that crosses the area bounded by the dotted contour shown in Fig. 1. Certainly line currents (henceforth referred to as source points since the analysis is two dimensional) at all points in the cross section contribute to the total flux, but due to the dimensions of the transmission line that are being considered, contributions from anti-symmetric source points (in the two films) distant from the observation point tend to cancel themselves out. It should be expected therefore, that virtually the entire net flux will be contributed by source points that lie within some small distance from the observation point (x,y) . This distance should be on the order of ℓ , the separation distance between the two films. Thus the kernel should be sharply peaked about $u = u'$ and, based on the discussion above, it should be expected that the magnitude of the kernel will be a monotonically decreasing function of $(|u-u'|)$. Since $\ell > d$ and

- $\frac{d}{2} \leq x, x' \leq \frac{d}{2}$, the two dimensional kernel in Eq. (9) is negative definite.

By considering the process by which Eq. (10) is derived from Eq. (9), it is apparent that the one-dimensional kernel in Eq. (10) is also negative definite.

A plot of the magnitude of the dimensionless kernel versus $(u-u')$ which summarizes the conclusions in the above discussion, is shown in Fig. 3. This approximate sketch is supported by numerical analysis and shows that the kernel drops off to $\approx \frac{1}{e}$ of its maximum value when $|u-u'| \approx \ell/W$, and that the bulk of the area under the curve (95%) is contained in the range $|u-u'|: 0 - 10 \frac{\ell}{W}$. Note that approximately 50% of the area under the curve is contained in the range $|u-u'|: 0 - \frac{\ell}{W}$. It might be pointed out here that the approximations in this and other sketches in the paper will not limit the accuracy of the final analytic results. The sketches are given as an aid to the reader and will be useful in determining the errors inherent in the analytic approximations to follow.

Letting $\lambda = \frac{(\beta d)^2 (w/d)}{8\pi}$, Eq. (10a) can be rewritten as

$$J(u) = C - \lambda \int_{-1}^{+1} J(u') \left| K(|u-u'|) \right| du' \quad (11)$$

Equation (11) can be solved by the Liouville-Neumann method of successive iterations: Let $J^{(0)}(u) = C$. Carrying through the integration in Eq. (11) yields

$$J^{(1)}(u) = C \left\{ 1 - \lambda \int_{-1}^{+1} \left| K(|u-u_1|) \right| du_1 \right\} \quad (12a)$$

Repeating the integration in Eq. (11), but now using $J^{(1)}(u')$ yields

$$J^{(2)}(u) = C \left\{ 1 - \lambda \int_{-1}^{+1} \left| K(|u-u_1|) \right| du_1 + \lambda^2 \int_{-1}^{+1} \int_{-1}^{+1} \left| K(|u_1-u_2|) \right| \left| K(|u-u_1|) \right| du_2 du_1 \right\} \quad (12b)$$

Thus, after n repetitions it can be shown that

$$J^{(n)}(u) = C \left\{ \sum_{m=0}^n (-\lambda)^m \int_{-1}^{+1} \int_{-1}^{+1} \cdots \int_{-1}^{+1} \left| K(|u_{m-1}-u_m|) \right| \cdots \left| K(|u-u_1|) \right| du_m \cdots du_1 \right\} \quad (12c)$$

Therefore the current density can be expressed as

$$J(u) = \lim_{n \rightarrow \infty} J^{(n)}(u) \quad (12d)$$

provided the series in Eq. (12c) converges as $n \rightarrow \infty$. The range of convergence for this series will be discussed later.

It is instructive to note that to zeroth order the current density, $J^{(0)}(u)$, is assumed to be uniform over the width of the film. The first order correction to this assumption, $J^{(1)}(u)$, is computed by considering the sum of the interactions of all the source points in the films on a particular observation point. This sum, $\lambda \int_{-1}^{+1} \left| K(|u-u_1|) \right| du_1$, will be referred to as the coupling factor $\lambda |K(u)|$. The second order correction, $J^{(2)}(u)$, is determined by considering the effect of all the source points on a particular source point before obtaining the coupling factor. The higher-order corrections are further expressions of the interactions of source points with source points. The coupling factor can be evaluated and shown to be

$$\lambda K(u) = I_1 \left| \begin{array}{l} \\ C=1 \end{array} \right. + \left(k - \frac{1}{2} \right) I_1 \left| \begin{array}{l} \\ C=2k-1 \end{array} \right. - \left(k + \frac{1}{2} \right) I_1 \left| \begin{array}{l} \\ C=2k+1 \end{array} \right. + 2I_2 \left| \begin{array}{l} \\ C=1 \end{array} \right. + I_2 \left| \begin{array}{l} \\ C=2k-1 \end{array} \right. - I_2 \left| \begin{array}{l} \\ C=2k+1 \end{array} \right. \quad (13a)$$

where $k = l/d$, and

$$I_{1/\lambda} = \ln \frac{[C^2(d/W)^2 + (u+1)^2]^{u+1}}{[C^2(d/W)^2 + (u-1)^2]^{u-1}} - 4 + 2C(d/W) \left\{ \tan^{-1} \frac{u+1}{C(d/W)} - \tan^{-1} \frac{u-1}{C(d/W)} \right\}, \text{ and}$$

$$I_{2/\lambda} = (1+u^2) (W/d) (\pi/2) - C^2(d/W) \left\{ \frac{1}{2} \left[\left(1 + \left[\frac{1+u}{C d/W} \right]^2 \right) \tan^{-1} \left(\frac{1+u}{C d/W} \right) + \left(1 + \left[\frac{1-u}{C d/W} \right]^2 \right) \tan^{-1} \left(\frac{1-u}{C d/W} \right) \right] - \frac{1}{C d/W} \right\} \quad (13b)$$

It is useful at this point to examine some of the properties of $K(u)$. Figure 4 shows the absolute magnitude of the kernel plotted against u' for various values of u . The area under each "u" curve is $|K(u)|$. Since the kernel is negative definite, $\kappa(u)$ is also negative definite. Due to the narrow effective width of the kernel (approximately $10(\frac{\ell}{W})$), it is seen that $K(u)$ is a weak function of u ($K(u) \approx K(o)$) in the central region of the film. When u is within $10(\frac{\ell}{W})$ of the edge of the film, $K(u)$ is a strong function of u , and in fact it can be shown that at the edges $|K(\pm 1)| = \frac{1}{2} |K(o)| + \epsilon$ where ϵ is a small positive number. These observations are summarized in Fig. 5.

Physically this implies that since an observation point is only affected by those source points within a range $\approx 10(\frac{\ell}{W})$, the observation points which are not within $10(\frac{\ell}{W})$ of the edges are effectively in an infinitely wide film. From Eq. (12d) and Fig. 5 it is seen that in this region $J(u)$ is a weak function of u (in an infinitely wide film J is independent of u). However, within $10(\frac{\ell}{W})$ of the edges, the observation point is affected by the presence of the edge of the film, and $J(u)$ is a strong function of u .

By considering a composite of Figs. 4 and 5 it is readily seen that

$$\int_{-1}^{+1} |K(u_1)| |K(|u-u_1|)| du_1 \approx |K(o)| |K(u)| \quad (14)$$

Thus in general

$$\int_{-1}^{+1} \int_{-1}^{+1} \cdots \int_{-1}^{+1} |K(|u_{m-1}-u_m|)| \cdots |K(|u-u_1|)| du_m \cdots du_1 \approx |K(o)|^{m-1} |K(u)| \quad (15)$$

Equations (14) and (15) are very nearly true in the central portion of the film. The error in the above approximations, when u is within $10(\frac{\ell}{W})$ of the film edges will be discussed in the next section. Combining Eqs. (12d) and (15) yields

$$J(u) = C \left\{ 1 - \lambda |K(u)| \left[\sum_{n=0}^{\infty} (-1)^n (\lambda |K(o)|)^n \right] \right\} \quad (16)$$

If $\lambda|\kappa(0)| < 1$ the series in Eq. (16) converges absolutely, and the current density distribution can be expressed in closed form as

$$J(u) = C \left\{ 1 - \frac{\lambda|\kappa(u)|}{1 + \lambda|\kappa(0)|} \right\} \quad (17)$$

Figure 6 indicates the range for the parameters d , W , and ℓ over which Eq. (16) converges. If $\lambda|\kappa(0)| \geq 1$ the series does not converge and the Liouville-Neumann method is not applicable. With the help of Fig. 5 an approximate normalized sketch of $J(u)$ versus u can be drawn (Fig. 7).

From Eq. (17) and the relation $\bar{H} = -\beta^{-2}(\nabla \times \bar{J})$, the x -component of the magnetic field can be shown to be

$$H_x(u) = \pm \frac{2C\lambda[K(1-u) - K(1+u)]}{\beta^2 W [1+\lambda|\kappa(0)|]} \quad (18)$$

where the plus and minus signs refer to the top and bottom films respectively. An approximate sketch of Eq. (18) is given in Fig. 8.

In principle, Ampere's law can be used to evaluate $H_y(x,u)$. However for the purposes of the discussion in the next section, only the form of H_y is necessary. In the central portion of the films it can readily be seen that H_y is maximum at $x = -\frac{d}{2}$, $-(\ell - \frac{d}{2})$ and approximately zero at $x = +\frac{d}{2}$, $-(\ell + \frac{d}{2})$.

ERROR ANALYSIS AND CONCLUSIONS

There are two sources of error in the analysis presented in the last section. The first error was introduced when it was assumed that the current density does not vary in the x -direction for the case $(\beta d) \leq 1$ (one dimensional approximation). The second error is associated with the approximations in Eqs. (14) and (15) (the edge approximations).

A. One Dimensional Approximation

In order to evaluate this error it is convenient to use a self consistency argument. In other words, the one dimensional solution, Eq. (17), is resubstituted

into the two-dimensional integral equation, Eq. (9), in order to find the x-direction variation of J . In practice it is more convenient to use the differential counterpart of Eq. (9), namely $\nabla^2 J = \beta^2 J$. The x-direction variation is then used to find an improved y-direction variation. For the purposes of this paper it is not important if J is not uniform in the x-direction, as long as the inclusion of this variation does not appreciably affect the y-direction variation. It is shown below that this is, in fact, the case.

From the discussion of the magnetic field distribution in the last section it is apparent that the largest x-direction variation of J occurs in the central portion of the film. This then is the worst case region as far as an error in the one-dimensional approximation is concerned. Using the self-consistent procedure outlined above, it is apparent that in the central region of the top film ($H_y(x = +\frac{d}{2}) \approx 0$)

$$J(x, y) \approx J(x) \approx J(0) \frac{\cosh \beta(x - d/2)}{\cosh \beta(d/2)} \quad (19)$$

It is seen that for $(\beta d) = 1$, $J(-\frac{d}{2}) \approx (1.5) J(\frac{d}{2})$. Thus there can be an appreciable x-direction variation. However, when Eq. (19) is substituted into Eq. (9) the improved y-variation integral equation is

$$J(u) = C - \alpha \lambda \int_{-1}^{+1} J(u') K(|u-u'|) du' \quad (20a)$$

where it can be shown that

$$1 < \alpha < \frac{\sinh \beta(d/2)}{\beta(d/2)} \quad (20b)$$

Thus, at worst, $\alpha = 1.04$ (for the case $\beta d = 1$) in the central region of the film. If $\lambda \rightarrow \alpha \lambda$ the magnitude of $J(u)$ in the central region is less than 2%, smaller than that predicted by Eq. (17). As was pointed out previously, this error is less near the film edges.

B. Edge Approximation

In order to evaluate the error in Eqs. (14) and (15) it is convenient to note that due to the properties of the kernel, which were discussed earlier,²

$$\int_{-1}^{+1} |\kappa(u')| |K(|u-u'|)| du' = |\kappa(0)| |\kappa(u)| [1 - \gamma(u)] \quad (21)$$

where $\gamma(u) \geq 0$. By considering more carefully the composite of Figs. 4 and 5 used to derive Eq. (14), it is seen that $\gamma(u)$ is largest when $u = \pm 1$, in which case $\gamma(\pm 1) \approx .25$. In the central portion of the film $\gamma(u) \approx 0$. Thus it is seen that at the film edges Eq. (14) is not very accurate. However, if Eqs. (12d) and (21) are used to derive a new expression for $J(\pm 1)$ it is found that

$$J(\pm 1) \approx C \left\{ 1 - \lambda |\kappa(1)| \left[1 - (.75) \lambda |\kappa(0)| + (.69) \lambda^2 |\kappa(0)|^2 - \frac{(.67)(\lambda|\kappa(0)|)^3}{1 + \lambda|\kappa(0)|} \right] \right\} \quad (22)$$

Thus $J(\pm 1)$ is less than 5% smaller than that predicted by Eq. (17) for all parameter values under consideration. This error is less near the center of the film.

If it is assumed that the superconducting films switch to the normally conducting state when J at any point in the films exceeds a critical value J_c , it is apparent that the switching is initiated at the film edges. From the error analysis it is clear that if the $J(u)$ given in Eq. (17) is used to calculate a critical current I_c (in terms of J_c), this value for the critical current will be smaller than the true critical current by less than 5%. It is noted that in calculating I_c the x-direction variation of J in the central portion of the film should be taken into account. This is easily done by combining Eqs. (17) and (19) as is done in the sample critical current calculation shown in the Appendix. J_c can be determined by making use of a microscopic theory,⁷ and/or by experimentally determining I_c for a particular choice of parameters which lie in the range defined above. Once J_c is known, I_c can be determined, using the above calculations for any other set of parameters which lie in the range under consideration in this paper.

ACKNOWLEDGEMENTS

The authors are grateful to P. Swigert for programming and carrying out the numerical calculations which were used to verify the results of this paper. Thanks are also due to G. Fair for several useful discussions.

APPENDIX

The critical current, I_c , of a superconducting strip transmission line, for the case $d/w \ll 1$, can easily be calculated. For this case, the current is uniform over a very large percentage of the film so that from Eq. (19) it can be shown that

$$I_o \approx J(0) W(\beta^{-1}) 2 \sinh (\beta d/2) \quad (A-1)$$

The dimensionless variable u will not be used in this section. From Eq. (17), and making use of the fact that $|\kappa(\pm w/2)| \approx \frac{1}{2} |\kappa(0)|$, it can be seen that

$$\frac{J(y = \pm \frac{W}{2})}{J(0)} \approx 1 + \frac{1}{2} \lambda |\kappa(0)| \quad (A-2)$$

where the variation of J in the x -direction at the film edges has been neglected in line with the discussion in the last section. According to the critical current density hypothesis $I_o = I_c$ when $J(\pm w/2) = J_c$. Using this hypothesis and combining Eqs. (A-1) and (A-2) yields

$$I_c = J_c W(\beta^{-1}) 2 \sinh (\beta d/2) / \left[1 + \frac{1}{2} \lambda |\kappa(0)| \right] \quad (A-3)$$

The numerator of the right-hand side of Eq. (A-3) is the critical current, I_{cu} , calculated on the assumption that the current density is uniform in the y -direction. It can be seen from Eq. (13) that

$$\left[\lambda |\kappa(0)| \right]_{d/w \ll 1} \approx \frac{(\beta d)^2}{2} \left(\frac{\lambda}{d} - \frac{1}{4} \right) \quad (A-4)$$

From Fig. 6 it is evident that Eq. (A-4) is satisfied for the case $d/w \leq .001$. It is interesting to note that in this range $\lambda \kappa(0)$ is independent of (d/w) . Therefore,

$$\frac{I_c}{I_{cu}} \approx \left[1 + \frac{(\beta d)^2}{4} \left(\frac{\lambda}{d} - \frac{1}{4} \right) \right]^{-1} \quad (A-5)$$

For situations in which (d/W) is not much less than unity, Eqs. (A-1) and (A-4) are not valid. In these cases the general expressions describing the variation of current density in the films can be used to calculate the critical current.

REFERENCES

1. J. C. Swihart, J. Appl. Phys., 32, 461 (1961)
2. N. H. Meyers, Proc. IRE, 494, 1640 (1961)
3. A. E. Brennemann, Proc. IRE, 51, ~~3~~^{#4}, 442 (1963)
4. A. E. Brennemann, J. J. McNichol, and D. P. Seraphim, Proc. IRE, 51, ~~7~~[#], 1009 (1963)
5. A. R. Sass, J. Appl. Phys., 35, 516 (1964)
6. A. R. Sass and F. J. Friedlaender, J. Appl. Phys., 35, 1494 (1964)
7. See for example J. Bardeen, Reviews of Modern Physics, 34, 667 (1962)
8. L. N. Cooper, Proceedings of the VII International Conference on Low Temperature Physics, 416 (1961)
9. P. M. Marcus, Proceedings of the VII International Conference on Low Temperature Physics, 418 (1961)

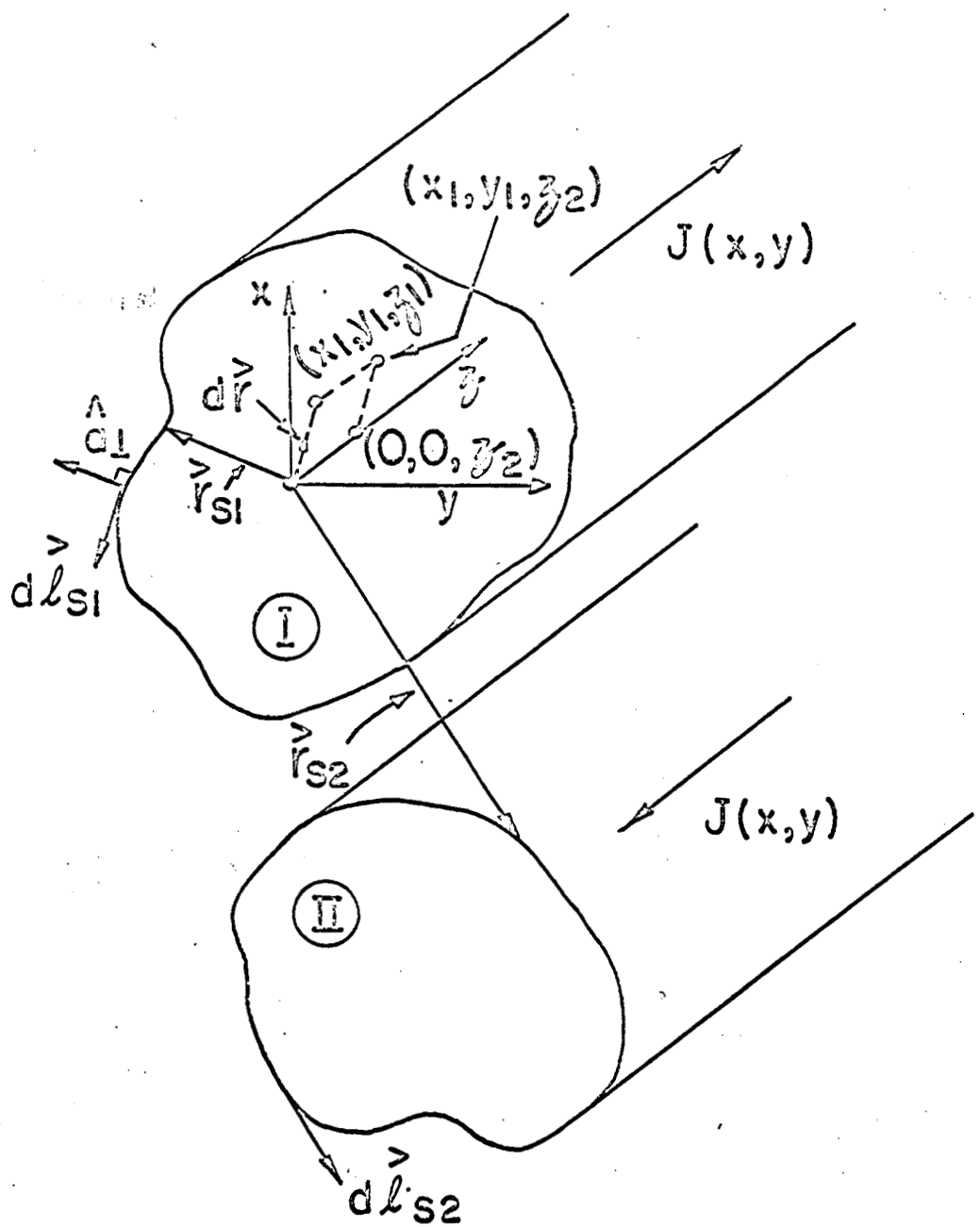


FIG. 1 PARALLEL CYLINDRICAL CONDUCTORS

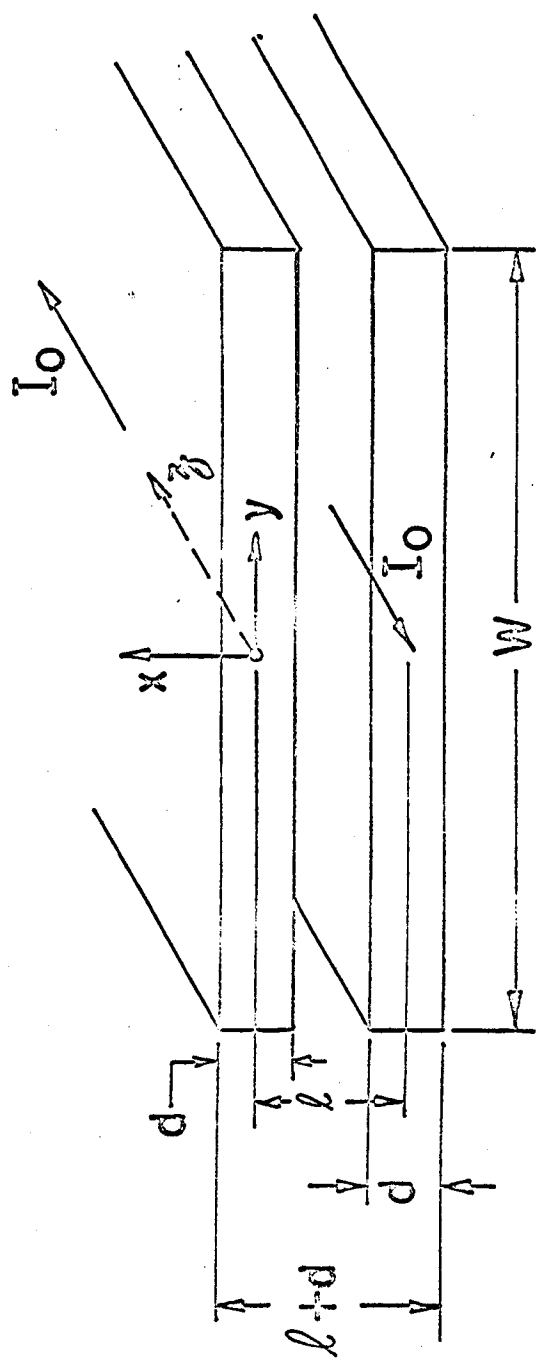


FIG. 2 STRIP TRANSMISSION LINE

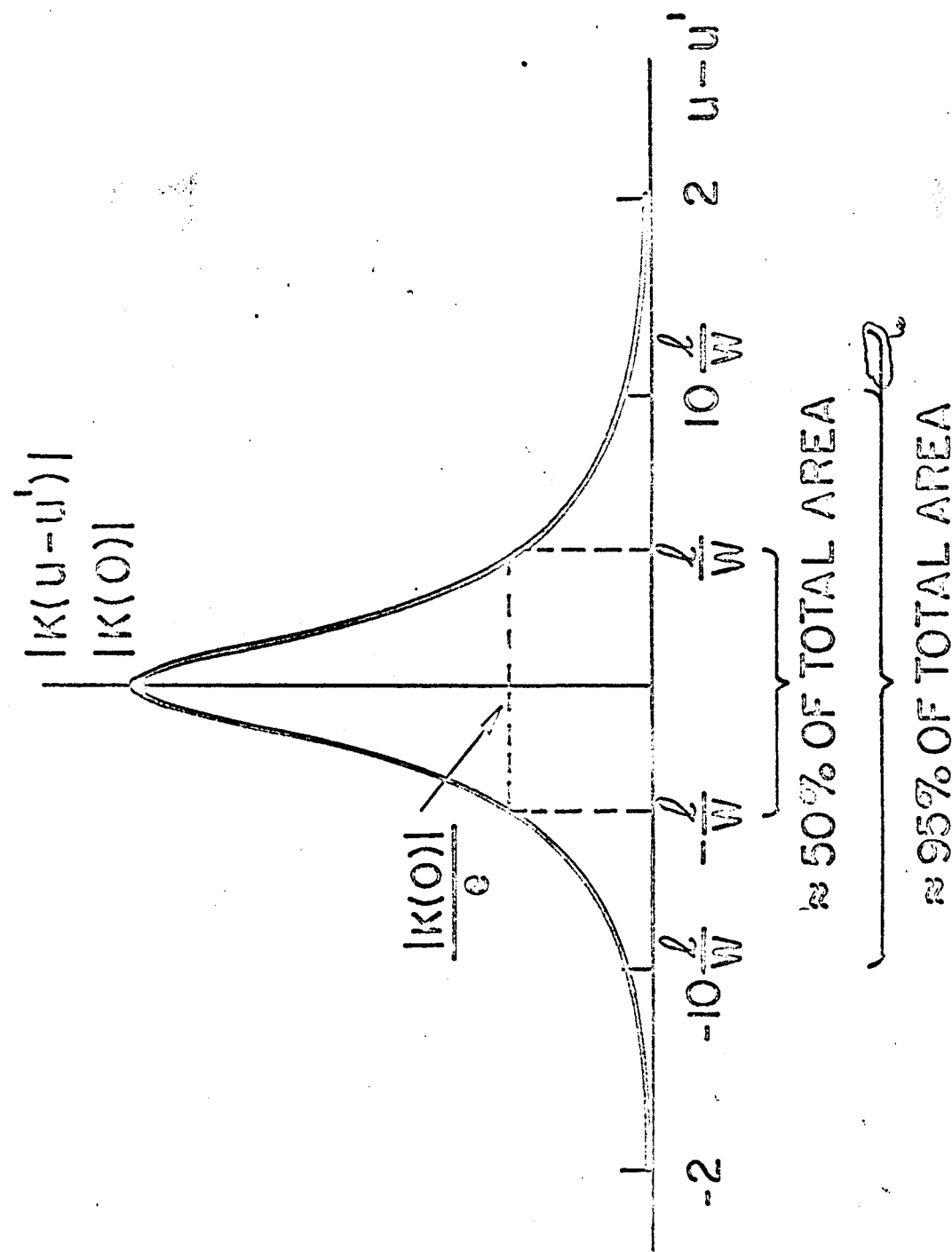


FIG. 3 KERNEL OF THE INHOMOGENEOUS INTEGRAL EQUATION (NOT TO SCALE)

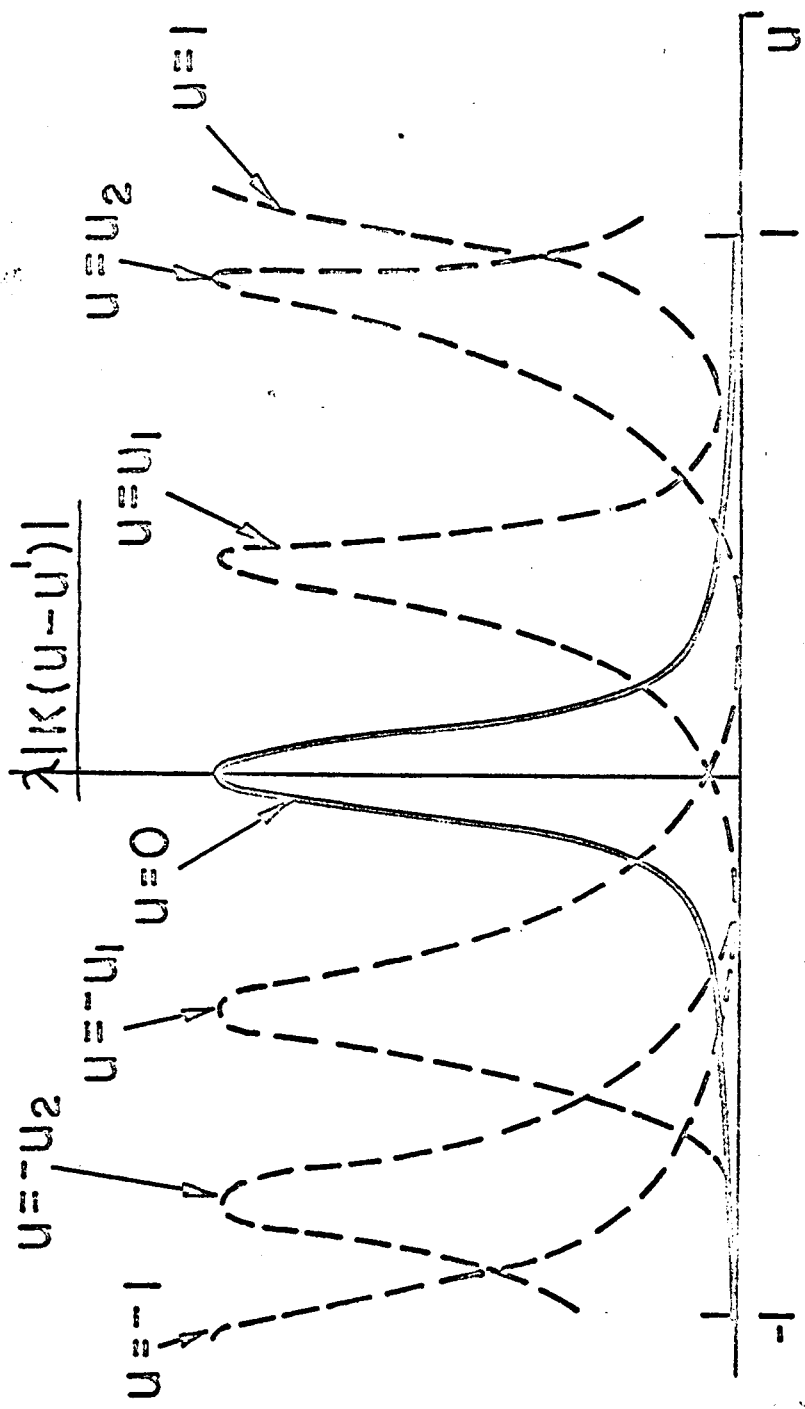


FIG. 4 DIFFERENTIAL COUPLING FACTOR (NOT TO SCALE)

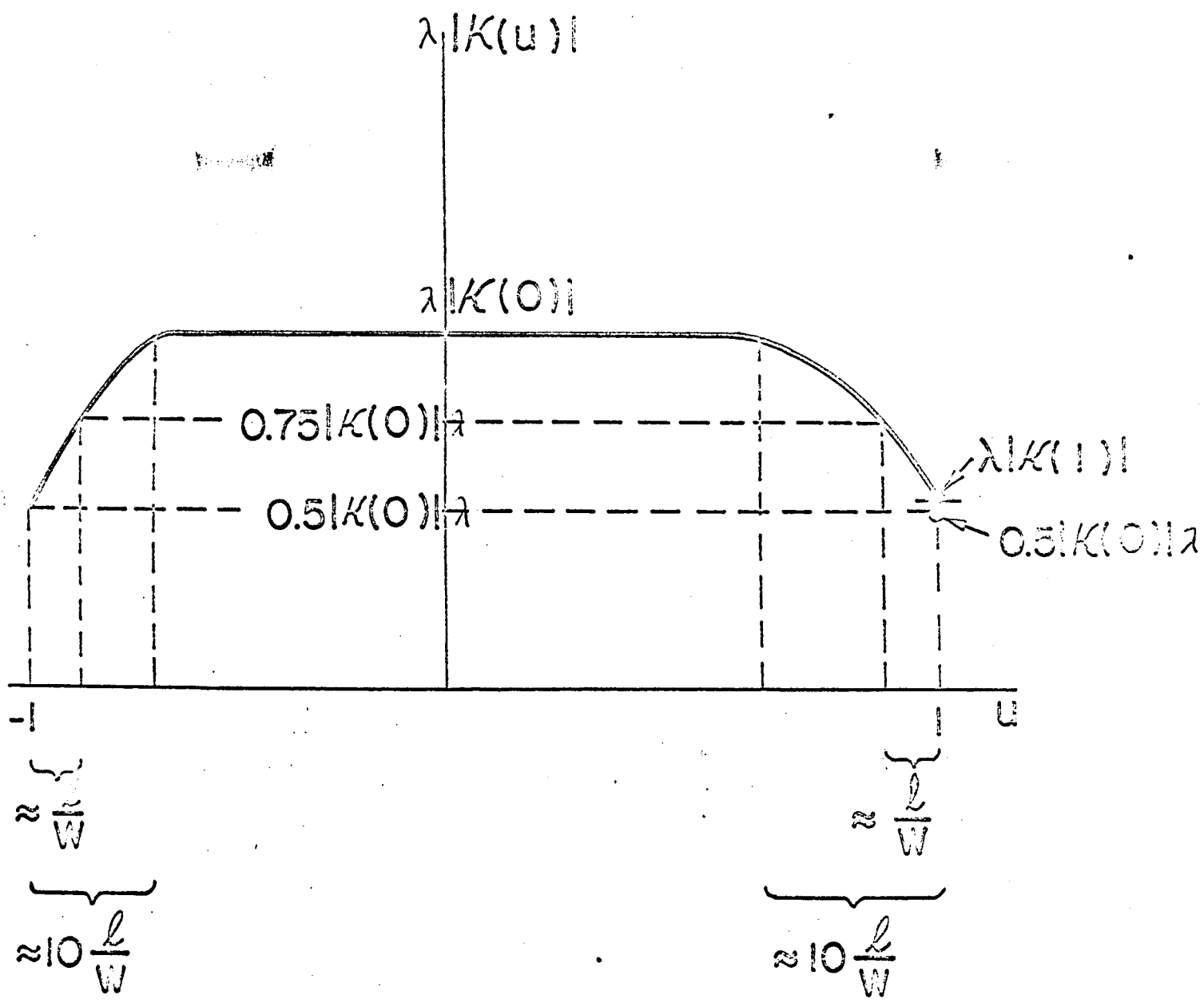


FIG.5 COUPLING FACTOR (NOT TO SCALE)

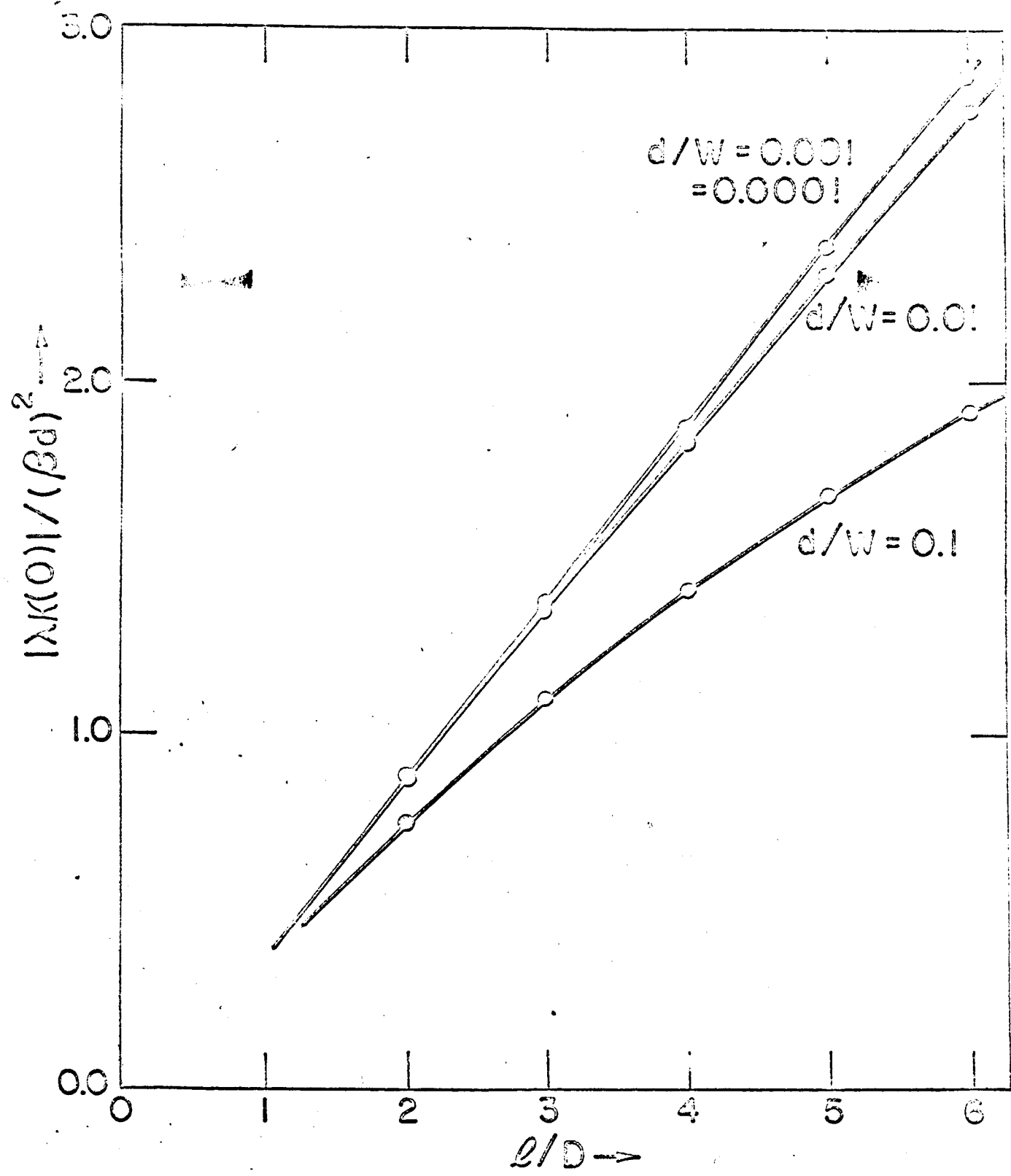
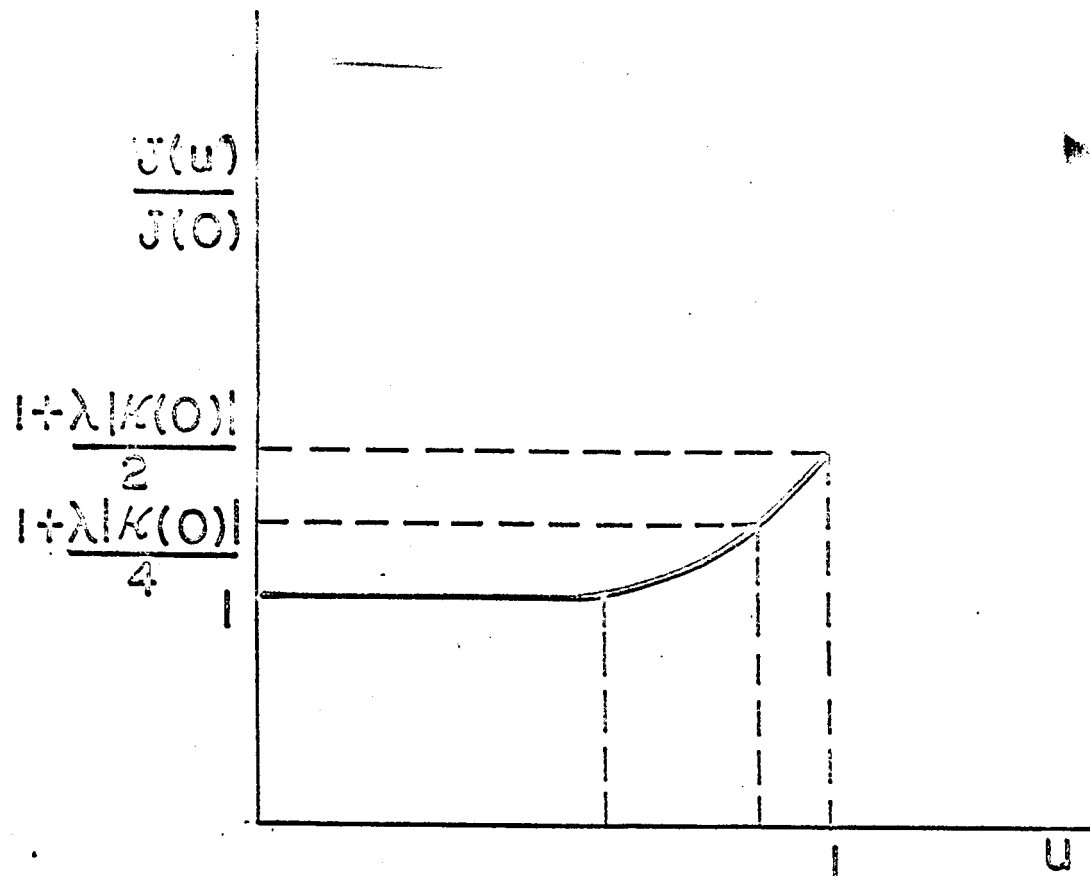


FIG. 6



$$\begin{aligned} &\approx \frac{\ell}{W} \\ &\approx 10 \frac{\ell}{W} \end{aligned}$$

FIG.7 CURRENT DISTRIBUTION (NOT TO SCALE)

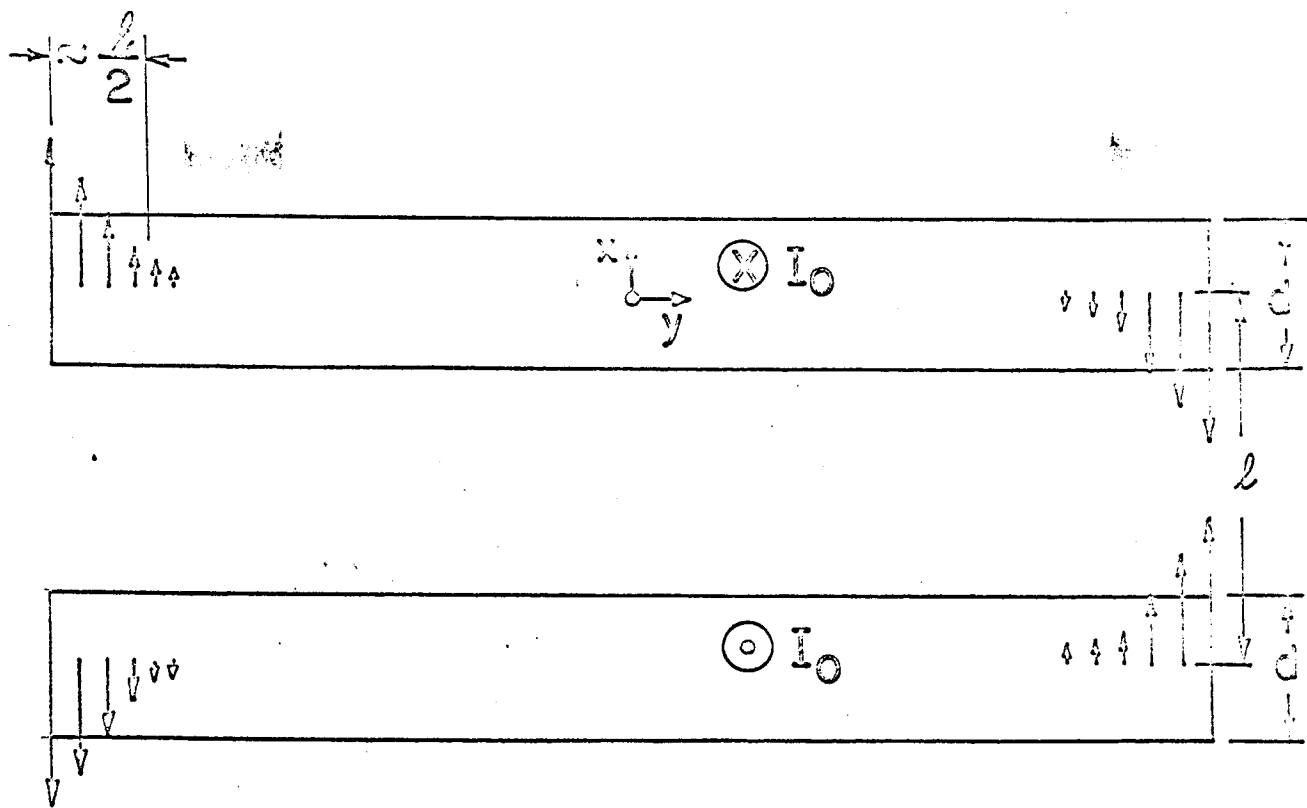


FIG.8 VERTICAL COMPONENT OF MAGNETIC FIELD(NOT TO SCALE)